11th World Congress on Computational Mechanics (WCCM XI)
5th European Conference on Computational Mechanics (ECCM V)
6th European Conference on Computational Fluid Dynamics (ECFD VI)
E. Oñate, J. Oliver and A. Huerta (Eds)

NONLINEAR DYNAMIC DEFORMATION OF A PIEZOELASTIC LAMINATED BEAM WITH FEEDBACK DAMPING MECHANISM

MASAYUKI ISHIHARA[*] AND YOSHIHIRO OOTAO[†]

[*] Graduate School of Engineering, Osaka Prefecture University (OPU)
1-1 Gakuen-cho, Naka-ku, Sakai-shi, Osaka 599-8531, Japan
e-mail: ishihara@me.osakafu-u.ac.jp

[†] Graduate School of Engineering, Osaka Prefecture University (OPU)
1-1 Gakuen-cho, Naka-ku, Sakai-shi, Osaka 599-8531, Japan
e-mail: ootao@me.osakafu-u.ac.jp

Key Words: *von Kármán Strain, Piezoelasticity, Vibration Control*

1 INTRODUCTION

Piezoelectric materials have been extensively used as sensors and actuators to suppress undesired vibration owing to their superior coupling effect between elastic and electric fields. Fiber reinforced plastics (FRPs) such as graphite/epoxy are in demand for constructing lightweight structures because they are lighter than most metals and have high specific strength. Structures composed of laminated FRP and piezoelectric materials are often called piezoelastic laminates and have attracted considerable attention in fields such as aerospace engineering and micro electro-mechanical systems. For aerospace applications, structures must be comparatively large and lightweight. Because of this, they are vulnerable to disturbances such as collisions with space debris. As a result, deformations due to these disturbances can be relatively large.

Therefore, dynamic problems involving large deformations of piezoelastic laminates have become the focus of several studies [1-3], in which Ishihara et al. analyzed vibration deviating arbitrarily from the equilibrium state and obtained the relationship between the deflection of the laminate and its velocity under various loading conditions. In these studies [1-3], methods to suppress undesired vibration due to known environmental causes were investigated; in other words, the manner of actuating, rather than the manner of sensing, was investigated.

In order to effectively suppress undesired vibration, it is important to consider both actuation and sensing and to integrate them into a feedback control system. Therefore, Ishihara et al. studied the control of the vibration of a piezoelastic laminate with a feedback control system under the framework of infinitesimal deformation [4-6]. However, as mentioned above, large deformation should be considered for applications of piezoelastic laminates.

In this study, therefore, we treat the control of the vibration with large amplitudes in a piezoelastic laminate with a feedback control system. The analytical model is a symmetric cross-ply laminated beam composed of fiber-reinforced laminae and two piezoelectric layers. The beam is simply supported at both edges, and it is subjected to an arbitrary initial

condition due to mechanical impact. The undesired vibration of the laminate is transformed into electric current by the direct piezoelectric effect in one of the piezoelectric layers, which serves as a sensor. Then, the electric voltage, with the magnitude of the current multiplied by a gain, is applied to the other piezoelectric layer which serves as an actuator. Large nonlinear deformation of the beam is analyzed on the basis of the von Kármán strain [7] and classical laminate theory. Equations of motion for the beam are derived using the Galerkin method [8]. As a result, the dynamic deflection of the beam is found to be governed by a Liénard equation [9]. Assuming a concrete profile of lamination, the equation is geometrically studied in order to reveal the essential characteristics of the beam and to investigate how to stabilize the dynamic deformation.

2 THEORETICAL ANALYSIS

2.1 Problem

The analytical model is a simply supported beam of dimensions $a \times b \times h$ and composed of N layers, as shown in Fig. 1. The k_s-th and k_a-th layers ($z_{k_s-1} \le z \le z_{k_s}$, $z_{k_a-1} \le z \le z_{k_a}$) exhibit piezoelectricity (with poling in the $+z$ or $-z$ direction), while the other layers do not. The beam is laminated in a symmetrical cross-ply manner. Mechanical disturbance is modeled as the combination of the initial deflection and velocity. The time variable is denoted by t.

To suppress the dynamic deformation due to the disturbance, the beam is subjected to the feedback control procedure: electric current $\dot{Q}_s(t)$ is detected in the k_s-th layer, which serves as a sensor; electrical potentials $\phi_{k_a-1}(t)$ and $\phi_{k_a}(t)$ determined on the basis of $\dot{Q}_s(t)$ are applied to the upper $\left(z = z_{k_a-1}\right)$ and lower $\left(z = z_{k_a}\right)$ surfaces, respectively, of the k_a-th layer, which serves as an actuator to suppress the deformation due to the disturbances. Moreover, in order to suppress the deformation effectively, the sensor and actuator are designed as a distributed sensor and actuator [10], i.e., the width of the electrodes for the k_s and k_a-th layers are variable as $b_s(x) = b \cdot f_s(x)$ and $b_a(x) = b \cdot f_a(x)$, respectively.

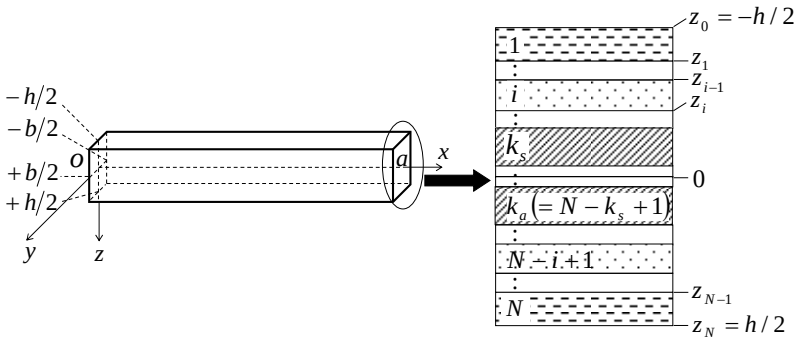

Figure 1: Analytical model

2.2 Governing equations

Based on the classical laminate theory, the displacements in the x and z directions are expressed, respectively, as

$$u = u^0(x,t) - z\frac{\partial w(x,t)}{\partial x}, \quad w = w(x,t), \tag{1}$$

where $u^0(x,t)$ and $w(x,t)$ denote the displacements on the central plane $(z=0)$. In order to treat nonlinear deformation, the von Kármán strain is introduced for the normal strain in the x direction as

$$\varepsilon_{xx} = \frac{\partial u}{\partial x} + \frac{1}{2}\left(\frac{\partial w}{\partial x}\right)^2 = \frac{\partial u^0}{\partial x} + \frac{1}{2}\left(\frac{\partial w}{\partial x}\right)^2 - z\frac{\partial^2 w}{\partial x^2}. \tag{2}$$

Assuming σ_{xx} and D_z denote the normal stress in the x direction and the electric displacement in the z direction, respectively, the constitutive equations for each layer are given as

$$\sigma_{xx} = E_i\varepsilon_{xx} - P_i(x)e_iE_z, \quad D_z = P_i(x)e_i\varepsilon_{xx} + \eta_iE_z, \tag{3}$$

where E_i, η_i, and e_i denote the elastic modulus, permittivity, and piezoelectric constant, respectively, in the i-th layer, and

$$e_{k_s} = e_{k_a}(\equiv -e_p < 0), \quad e_i = 0 \ (i \neq k_a \text{ and } i \neq k_s). \tag{4}$$

The function $P_i(x)$ takes values of +1 and -1 in the portions with poling in the $+z$ and $-z$ directions, respectively.

By substituting Eq. (2) into Eq. (3)-1 and integrating the result, without and with z multiplied, for $-h/2 \le z \le h/2$, we have the constitutive equations of the laminated beam as

$$N_x = A\left[\frac{\partial u^0}{\partial x} + \frac{1}{2}\left(\frac{\partial w}{\partial x}\right)^2\right] - N_x^E, \quad M_x = -D\frac{\partial^2 w}{\partial x^2} - M_x^E, \tag{5}$$

where N_x and M_x denote the resultant force and moment, respectively; A and D denote the extensional and bending rigidities, respectively; and N_x^E and M_x^E denote the electrically induced resultant force and moment, respectively, per unit width. By considering $b_s(x) = b \cdot f_s(x)$ and $b_a(x) = b \cdot f_a(x)$, N_x^E and M_x^E are, respectively, defined by

$$\left.\begin{aligned} N_x^E &= \left[P_{k_a}(x)f_a(x)\right]\cdot e_{k_a}\int_{z_{k_a-1}}^{z_{k_a}} E_z\mathrm{d}z + \left[P_{k_s}(x)f_s(x)\right]\cdot e_{k_s}\int_{z_{k_s-1}}^{z_{k_s}} E_z\mathrm{d}z, \\ M_x^E &= \left[P_{k_a}(x)f_a(x)\right]\cdot e_{k_a}\int_{z_{k_a-1}}^{z_{k_a}} E_z z\mathrm{d}z + \left[P_{k_s}(x)f_s(x)\right]\cdot e_{k_s}\int_{z_{k_s-1}}^{z_{k_s}} E_z z\mathrm{d}z \end{aligned}\right\}. \tag{6}$$

Equations of motion for the laminated beam are given as

$$\frac{\partial N_x}{\partial x}=0,\quad \frac{\partial^2 M_x}{\partial x^2}+N_x\frac{\partial^2 w}{\partial x^2}=\rho h\frac{\partial^2 w}{\partial t^2}+ch\frac{\partial w}{\partial t}, \tag{7}$$

where ρ denotes the mass density averaged along the thickness direction. $c(\geq 0)$ denotes the damping coefficient which is inherent in the beam without the feedback system.

By substituting Eqs (5) into Eqs (7), we have the equations which govern displacements u^0 and w as

$$L_1(u^0,w)=\frac{\partial N_x^E}{\partial x},\quad \rho h\frac{\partial^2 w}{\partial t^2}+ch\frac{\partial w}{\partial t}+L_2(u^0,w)=-\frac{\partial^2 M_x^E}{\partial x^2}-N_x^E\frac{\partial^2 w}{\partial x^2}, \tag{8}$$

where the definitions of differentiation operators L_1 and L_2 are given as

$$L_1(u^0,w)=A\left(\frac{\partial^2 u^0}{\partial x^2}+\frac{\partial w}{\partial x}\frac{\partial^2 w}{\partial x^2}\right),\quad L_2(u^0,w)=-A\left[\frac{\partial u^0}{\partial x}+\frac{1}{2}\left(\frac{\partial w}{\partial x}\right)^2\right]\frac{\partial^2 w}{\partial x^2}+D\frac{\partial^4 w}{\partial x^4}. \tag{9}$$

Because the beam is simply supported at both edges, the mechanical boundary conditions are expressed as

$$u^0=0,\ w=0,\ M_x=0;\ x=0,a. \tag{10}$$

By assuming the thicknesses of the k_s-th and k_a-th layers are sufficiently small compared to its length a and considering Eqs (4) and (6), we have

$$\left.\begin{aligned} N_x^E &= -\left[P_{k_a}(x)f_a(x)\right]\cdot e_{k_a}\left[\phi_{k_a}(t)-\phi_{k_a-1}(t)\right]-\left[P_{k_x}(x)f_s(x)\right]\cdot e_{k_s}\left[\phi_{k_s}(t)-\phi_{k_s-1}(t)\right],\\ M_x^E &= -\left[P_{k_a}(x)f_a(x)\right]\cdot e_{k_a}\left[\phi_{k_a}(t)-\phi_{k_a-1}(t)\right]\frac{z_{k_a}+z_{k_a-1}}{2}\\ &\quad -\left[P_{k_x}(x)f_s(x)\right]\cdot e_{k_s}\left[\phi_{k_s}(t)-\phi_{k_s-1}(t)\right]\frac{z_{k_s}+z_{k_s-1}}{2} \end{aligned}\right\}, \tag{11}$$

where $\phi_{k_s-1}(t)$ and $\phi_{k_s}(t)$ denote electrical potentials on the upper $(z=z_{k_s-1})$ and lower $(z=z_{k_s})$ surfaces, respectively, of the k_s-th layer

2.3 Sensor equation

By considering $b_s(x)=b\cdot f_s(x)$, the detected electric charge $Q_s(t)$ is evaluated by

$$Q_s(t)=\frac{1}{2}\left[\int_0^a (D_z)_{z=z_{k_s-1}}\, b\cdot f_s(x)\mathrm{d}x+\int_0^a (D_z)_{z=z_{k_s}}\, b\cdot f_s(x)\mathrm{d}x\right]. \tag{12}$$

By substituting Eqs (2) and (3)-2 into Eq. (12), differentiating the result with respect to t, and applying the *virtual short condition* [10],

$$\phi_{k_s}(t)=\phi_{k_s-1}(t), \tag{13}$$

we have

$$\dot{Q}_s(t)=\int_0^a e_{k_s} b\left[\frac{\partial \dot{u}^0}{\partial x}+\frac{\partial w}{\partial x}\frac{\partial \dot{w}}{\partial x}-\frac{z_{k_s}+z_{k_s-1}}{2}\frac{\partial^2 \dot{w}}{\partial x^2}\right]\left[P_{k_s}(x)f_s(x)\right]\mathrm{d}x\,. \tag{14}$$

2.4 Galerkin method

The Galerkin method [8] is used to solve Eqs (8) under the condition described by Eqs (10). In order to extract the fundamental physical characteristics of the dynamic behavior, the most fundamental mode is treated as

$$u^0=u_1(t)\sin\alpha x,\quad w=w_1(t)\sin\alpha x\,;\quad \alpha\equiv\pi/a\,. \tag{15}$$

Moreover, in order to construct the modal sensor and actuator which are effective against the mode described by Eqs (15), the profiles of poling direction and the widths of the electrodes are designed to be

$$\left[P_{k_a}(x)f_a(x)\right]=\left[P_{k_s}(x)f_s(x)\right]=\sin\alpha x\,. \tag{16}$$

Then, the Galerkin method is applied to Eqs (8) to obtain

$$\left.\begin{aligned}&\int_0^a\left[L_1\left(u^0,w\right)-\frac{\partial N_x^E}{\partial x}\right]\sin\alpha x\,\mathrm{d}x=0,\\&\int_0^a\left[\rho h\frac{\partial^2 w}{\partial t^2}+ch\frac{\partial w}{\partial t}+L_2\left(u^0,w\right)+\frac{\partial^2 M_x^E}{\partial x^2}+N_x^E\frac{\partial^2 w}{\partial x^2}\right]\sin\alpha x\,\mathrm{d}x=0\end{aligned}\right\}. \tag{17}$$

Substituting Eqs (4), (11), (13), (15), and (16) into Eqs (17) and (14) gives

$$u_1=0,\quad \rho h\frac{\mathrm{d}^2 w_1}{\mathrm{d}t^2}+ch\frac{\mathrm{d}w_1}{\mathrm{d}t}+\left(k_L+k_A\right)w_1+k_N w_1^3=p_A,\ \dot{Q}_s(t)=-e_p b\frac{2a}{\pi}\alpha^2\left(\frac{w_1}{3}-\frac{\pi}{4}z_p\right)\dot{w}_1, \tag{18}$$

where

$$\left.\begin{aligned}&k_L=D\alpha^4,\quad k_A=-\frac{8}{3\pi}\alpha^2 e_p\left[\phi_{k_a}(t)-\phi_{k_a-1}(t)\right],\quad k_N=\frac{1}{8}A\alpha^4,\\&p_A=\alpha^2 e_p\left[\phi_{k_a}(t)-\phi_{k_a-1}(t)\right]z_p,\quad z_p=\frac{z_{k_a}+z_{k_a-1}}{2}\end{aligned}\right\}. \tag{19}$$

2.5 Equation for feedback control

We consider that the electric voltage applied to the actuator, $\left[\phi_{k_a}(t)-\phi_{k_a-1}(t)\right]$, is designed to be proportional to the electric current detected by the sensor, $\dot{Q}_s(t)$, as

$$\phi_{k_a}(t)-\phi_{k_a-1}(t)=-G\dot{Q}_s(t), \tag{20}$$

where G denotes the gain of the feedback control.

By substituting Eq. (20) into Eqs (18) and (19), we have

$$\left.\begin{aligned}&\rho h\frac{\mathrm{d}^2 w_1}{\mathrm{d}t^2}+ch\frac{\mathrm{d}w_1}{\mathrm{d}t}+\left[D\alpha^4+G\frac{8}{3\pi}\alpha^2 e_p\dot{Q}_s(t)\right]w_1+\frac{A\alpha^4}{8}w_1^3=-G\alpha^2 e_p\dot{Q}_s(t)z_p,\\&\dot{Q}_s(t)=e_p b\frac{2a}{\pi}\left(\frac{\pi}{4}z_p-\frac{1}{3}w_1\right)\alpha^2\dot{w}_1\end{aligned}\right\},\qquad(21)$$

where z_p defined by Eq. (19)-5 denotes the z coordinate of the central plane of the actuator. By eliminating $\dot{Q}_s(t)$ in Eqs (21) and introducing the nondimensional quantities as

$$W\equiv\frac{w_1}{h},\ \ \tau\equiv\sqrt{\frac{hA\alpha^4}{8\rho}}t,\ \ \lambda\equiv\frac{8D}{h^2A},\ \ \delta\equiv\frac{4c}{\alpha^2\sqrt{2\rho hA}},\ \ \zeta_p\equiv\frac{z_p}{h},\ \ \gamma\equiv\frac{8}{A}e_p^2 ab\sqrt{\frac{hA\alpha^4}{8\rho}}G,\qquad(22)$$

we have

$$\frac{\mathrm{d}^2 W}{\mathrm{d}\tau^2}+\delta\frac{\mathrm{d}W}{\mathrm{d}\tau}+\gamma\frac{1}{2}\left(\zeta_p+\frac{8}{3\pi}W\right)\left(\zeta_p-\frac{4}{3\pi}W\right)\frac{\mathrm{d}W}{\mathrm{d}\tau}+\lambda W+W^3=0.\qquad(23)$$

Thus, from Eqs (22) and (23), it is found that the nondimensional deflection W is governed by nondimensional parameters λ, δ, ζ_p $\left(-1/2<\zeta_p<1/2\right)$, and γ, which denote the rigidity, damping coefficient, position of the actuator, and gain, respectively. It is found that Eq. (23) has a sole equilibrium solutions $W=0$.

In order to extract the governing parameters, nondimensional quantities are introduced as

$$x\equiv\frac{W}{\sqrt{\lambda}},\ \ t\equiv\sqrt{\lambda}\tau,\ \ \varepsilon\equiv\frac{\delta}{\sqrt{\lambda}}(\geq 0),\ \ \mu\equiv\sqrt{\lambda}\gamma,\ \ z\equiv\frac{3\pi}{16}\frac{\zeta_p}{\sqrt{\lambda}},\qquad(24)$$

where x, t, ε, μ, and z denote the nondimensional quantities of the deflection, time, damping coefficient, gain, and actuator's position, respectively. Hereafter, x, z, and t are employed in the sense of Eqs (24) for brevity. Then, Eq. (23) is nondimensionalized as

$$\frac{\mathrm{d}^2 x}{\mathrm{d}t^2}+\left[\varepsilon+\mu f(x,z)\right]\frac{\mathrm{d}x}{\mathrm{d}t}+g(x)=0,\qquad(25)$$

where functions $f(x,z)$ and $g(x)$ are defined as

$$f(x,z)\equiv-\frac{16}{9\pi^2}(x+2z)(x-4z),\ \ g(x)=x+x^3.\qquad(26)$$

Equation (25) is known as Liénard's equation [9]. In Eq. (25), ε represents the damping effect inherent in the beam without the feedback system, and $\mu f(x,z)$ represents the effect derived from the feedback control system. The former generally contributes to stabilization of the vibration. The latter may stabilize or destabilize the vibration because the sign of $f(x,z)$ may change during the operation.

From Eqs (25) and (26), it is found that Eq. (25) has its sole equilibrium solution $x=0$. We call the function $f(x,z)$ as the damping characteristic function in the sense that it describes the dependency of the damping intensity for a deflection From Eq. (26), it is found

that

$$f(x,z)>0 \text{ for } -2z<x<4z\,. \tag{27}$$

For $\mu>0$, therefore, the equilibrium solution $x=0$ is expected to be globally stable within a certain range around $x=0$. Conversely, from Eqs (26), it is expected that a vibration with relatively large amplitude will be unstable.

In order to determine the range of deformation in which the system is operated stably, Eq. (25) is analyzed geometrically by introducing the Liénard's phase plane [11] (x,y) that is governed by

$$\dot{x}=\mu\left[y-F(x,z)\right]-\varepsilon x,\ \dot{y}=-\frac{1}{\mu}g(x), \tag{28}$$

where the overdot denotes differentiation with respect to t, and $F(x,z)$ is defined by

$$F(x,z)\equiv\int_0^x f(x,z)\mathrm{d}x=-\frac{16}{27\pi^2}x\left(x+\frac{\sqrt{105}-3}{2}z\right)\left(x-\frac{\sqrt{105}+3}{2}z\right). \tag{29}$$

From the first part of Eqs (28), we have

$$y=\frac{\dot{x}}{\mu}+F(x,z)+\frac{\varepsilon x}{\mu}. \tag{30}$$

Thus, we call y the *modified velocity* in the sense that it is related to the *actual velocity* $\dot{x}$.

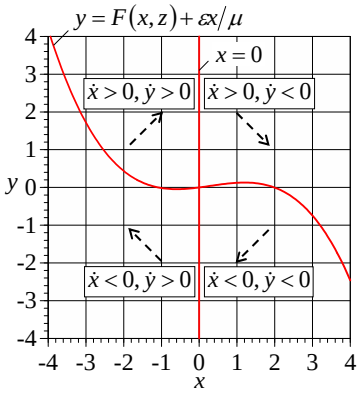

Figure 2: Characteristics of phase plane $(z=0.3,\ \varepsilon=0)$

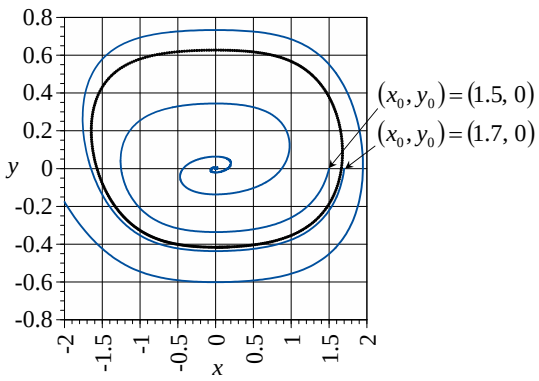

Figure 3: Examples of trajectories $(\mu=5,\ z=0.3,\ \varepsilon=0)$

Figure 2 shows the characteristics of the phase plane governed by Eq. (28). The solid lines in red denote

$$x=0,\ y=F(x,z)+\frac{\varepsilon x}{\mu}, \tag{31}$$

which make the right-hand sides of Eqs (28) null and are, therefore, called *nullclines*. From

Eqs (28), it is found that the nullclines in Eqs (31) divide the phase plane shown in Fig. 2 into four parts by the signs of $\dot{x}$ and $\dot{y}$. The broken arrows in Fig. 2 denote the directions of the trajectories governed by Eqs (28). The examples of the trajectories are indicated by blue lines in Fig. 3. The point (x_0, y_0) denotes the initial combination of (x, y). From Fig. 3, it is found that a trajectory may move toward or away from the equilibrium point $(x, y) = (0,0)$; in other words, the vibration may be stable or unstable. Therefore, it is expected that there is a closed boundary line that divides the stability as indicated by the broken line in Fig. 3. Such a line is usually called the *limit cycle*. It should be noted that the limit cycle is dependent on parameters μ, z, and ε.

3 NUMERICAL RESULTS

We consider that the piezoelectric layers are of $BaTiO_3$ and other layers are of graphite/epoxy (GE). Their material constants are given in [6]. We consider that the layers are piled as shown in Fig. 4 with poling in the $+z$. The length of the beam chosen as $a/h = 100$. Under these conditions, the nondimensional quantity of the actuator position is calculated at $z = 0.204$ and parameter μ is variable. To be on the safe side, we exclude the damping effect inherent in the beam as $\varepsilon = 0$, and include the damping effect derived from the feedback control system only. In that case, Eq. (25) combined with Eqs (26) is invariant under $x \to -x$ and $z \to -z$ or under $t \to -t$ and $\mu \to -\mu$, the case of $z \geq 0$ and $\mu \geq 0$ is treated. As stated in Subsection 2.5, the limit cycle divides the stability in the phase plane. Therefore, it is important to investigate the shape of the limit cycle.

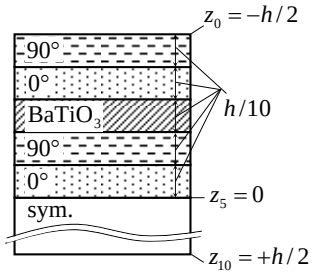

Figure 4: Cross-section of beam

Figures 5 (a)-(d) show the limit cycles for various values of μ, in which the blue solid lines and red broken lines denote the limit cycles and the nullclines determined by Eqs (31), respectively. In Fig. 5, the limit cycles are found to be horizontal $(\mathrm{d}y/\mathrm{d}x = \dot{y}/\dot{x} = 0)$ or vertical $(\mathrm{d}x/\mathrm{d}y = \dot{x}/\dot{y} = 0)$ on the nullclines, which is found also from Eqs (28) and (31). Moreover, as shown in Fig. 2, the abscissa or the ordinate of a limit cycle becomes maximum or minimum on the nullclines. From Fig. 5, it is found that, as the value of μ increases, the shape of the limit cycle converges to the shape shown in Fig. 5 (d).

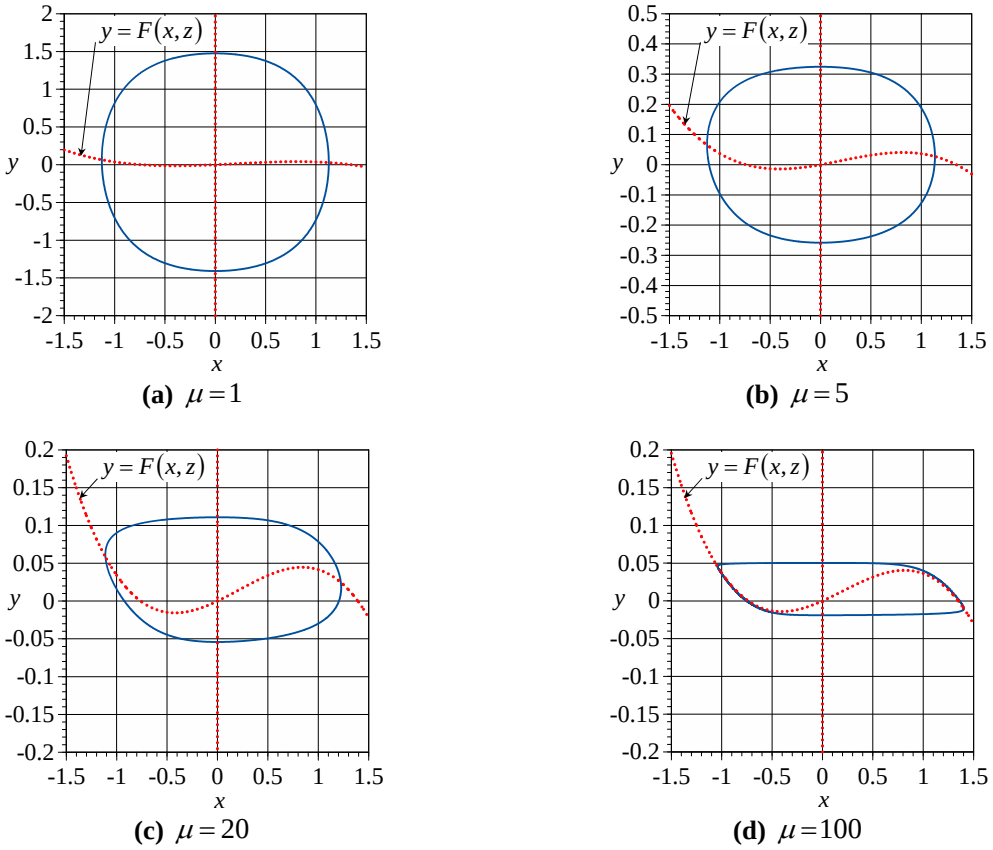

Figure 5: Effect of gain on limit cycle $(z = 0.204)$

The maximum and minimum values of the abscissa and ordinate of a limit cycle are important characteristics of the cycle because they correspond to the limit within which the system is operated safely. To be more precise, the maximum and minimum values of the abscissa correspond to the upper and lower limits of the initial position when the initial *modified velocity* is zero, and those of the ordinate correspond to the upper and lower limits of the initial *modified velocity* when the initial position is zero. In view of these facts, we refer to the maximum and minimum values of the abscissa of a limit cycle as the upper and lower limits of the initial position, respectively, and refer to those of the ordinate of the cycle as the upper and lower limits of the initial *modified velocity*, respectively. In addition, we refer to the maximum and minimum values of the *actual velocity* $\dot{x}$ along the limit cycle as the upper and lower limits of the *actual velocity*, respectively.

Figure 6 shows the variations of the upper and lower limits of the position, *modified velocity*, and *actual velocity* with parameter μ, in which subscripts "upper" and "lower" correspond to the upper and lower limits, respectively. From Figs 6 (a) and (b), it is found that, as μ increases, the upper and lower limits of the position and *modified velocity* change monotonically and converge to certain values. From Fig. 6 (c), it is found that the upper limit of the *actual velocity* increases as μ increases and that the lower limit has a local maximum.

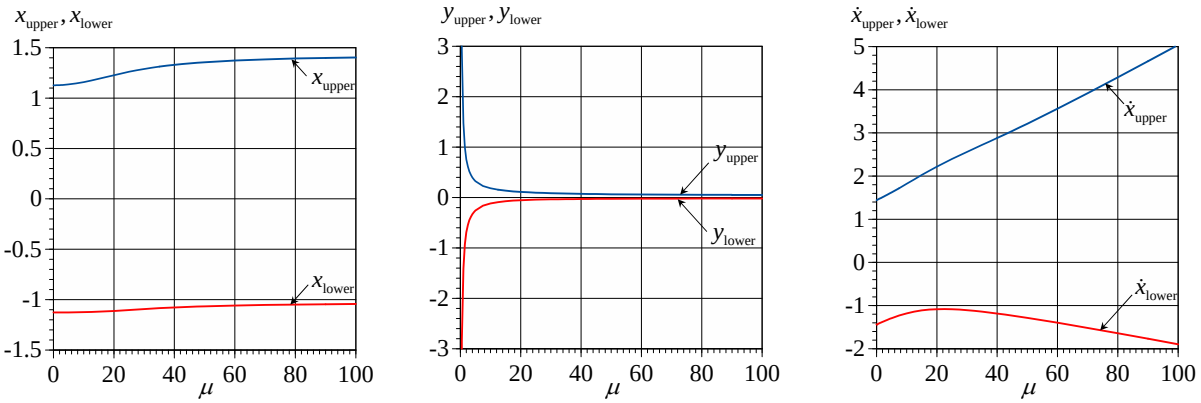

(a) Position **(b)** Modified velocity **(d)** Actual velocity

Figure 6: Variations of upper and lower limits with gain $(z = 0.204)$

Usually, a larger value of μ is preferable in order to quickly pull the system back to the equilibrium point $(x, y) = (0,0)$. However, as shown in x_{lower} in Fig. 6 (a), the limit within which the system is operated safely may decrease. In this regard, the safe ranges of the initial position x_{initial}, *modified velocity* y_{initial}, and *actual velocity* $\dot{x}_{\text{initial}}$ are investigated. From Fig. 6, it is found that the system is stable for an arbitrary value of μ when x_{initial}, y_{initial}, and $\dot{x}_{\text{initial}}$ satisfy $x_{\text{lower}}(\mu >> 1) < x_{\text{initial}} < x_{\text{upper}}(\mu = 0)$, $y_{\text{lower}}(\mu >> 1) < y_{\text{initial}} < y_{\text{upper}}(\mu >> 1)$, and $\dot{x}_{\text{lower}}(\mu \cong 22.5) < \dot{x}_{\text{initial}} < \dot{x}_{\text{upper}}(\mu = 0)$, respectively.

4 CONCLUSIONS

- The control of the free vibration with large amplitude in a piezoelastic laminated beam subjected to an arbitrary initial condition with a feedback control system was treated.
- Th beam was found to be governed by a Liénard equation dependent on the gain of the feedback control and the configuration of the actuator.
- The equation was analyzed geometrically by the Liénard's phase plane, and the essential characteristics of the beam and stabilization of the dynamic deformation were clearly demonstrated.

REFERENCES

[1] Ishihara, M. and Noda, N. Non-linear dynamic behaviour of a piezothermoelastic laminate. *Philosophical Magazine* (2005) **85**:4159-4179.

[2] Watanabe, Y., Ishihara, M., and Noda, N. Nonlinear transient behavior of a piezothermoelastic laminated beam subjected to mechanical, thermal and electrical load. *Journal of Solid Mechanics and Materials Engineering* (2009) **3**:758-769.

[3] Ishihara, M., Watanabe Y., and Noda, N. Non-linear dynamic deformation of a piezothermoelastic laminate. in Irschik, H., Krommer, M., Watanabe, K., and Furukawa, T. (Ed.). *Mechanics and model-based control of smart materials and structures*. Springer-Verlag, (2010).

[4] Ishihara, M., Noda, N., and Morishita, H. Control of dynamic deformation of a piezoelastic beam subjected to mechanical disturbance by using a closed-loop control system. *Journal of Solid Mechanics and Materials Engineering* (2007) **1**:864-874.
[5] Ishihara, M., Morishita, H., and Noda, N. Control of dynamic deformation of a piezothermoelastic beam with a closed-loop control system subjected to thermal disturbance. *Journal of Thermal Stresses* (2007) **30**:875-888.
[6] Ishihara, M., Morishita, H., and Noda, N. Control of the transient deformation of a piezoelastic beam with a closed-loop control system subjected to mechanical disturbance considering the effect of damping. *Smart Materials and Structures* (2007) **16**:1880-1887.
[7] Chia, C. Y. *Nonlinear analysis of plates*. McGraw-Hill, (1980).
[8] Fletcher, C. A. J. *Computational Galerkin method*. Springer, (1984).
[9] Strogatz, S. H. *Nonlinear dynamics and chaos*. Westview Press, (2001).
[10] Lee, C. -K. Piezoelectric laminates: Theory and experiments for distributed sensors and actuators. in Tzou H. S. and Anderson G. L. (Ed.). *Intelligent Structural Systems*. Kluwer Academic Publishers, (1992).
[11] Minorsky, N. *Nonlinear Oscillations*. Van Nostrand, (1962).